Electronic Supplementary Material (ESI) for Nanoscale.

SUPPLEMENTARY INFORMATION

Intracellular Targeted Delivery of Quantum Dots with Extraordinary Performance Enabled Novel Nanomaterial Design

Jun Wang, Jie Dai, Xuan Yang, Xiaoya Yu, Steven R. Emory, Xueqing Yong, Jinhua Xu, Ling Mei, Jinbing Xie, Ning Han, Xuejin Zhang, Gang Ruan

Corresponding author: Gang Ruan, gangruan@nju.edu.cn.

This Supplementary Information file contains the following:

Supplementary Table 1.

Supplementary Figures 1-10.

Descriptions of Supplementary Videos 1-3.

Supplementary Table 1 Critical analysis of representative efforts in the literature on intracellular targeted delivery of quantum dots (QDs)

Publications	**Contents**	**Comments/limitations**
➢ Kairdolf, B.A. *et al.* Semiconductor quantum dots for bioimaging and biodiagnostic applications. *Annu. Rev. Anal. Chem.* **6,** 143-162 (2013). ➢ Kairdolf, B.A., Qian, X. & Nie, S.M. Bioconjugated nanoparticles for biosensing, in vivo imaging, and medical diagnostics. *Anal.Chem.* **89,** 1015-1031 (2017).	These two recent reviews from the same research group summarize the techniques and highlight the challenges of intracellular targeted delivery of QDs.	These reviews point out that intracellular targeting of QDs is a key challenge for QD-based biotechnologies.
➢ Pinaud, F., Clarke, S., Sittner, A. & Dahan, M. Probing cellular events, one quantum dot at a time. *Nat. Methods* **7,** 275-285 (2010).	This review summarizes the progress and challenges of using QDs for imaging and tracking in biological cells.	This review states that the most important open challenge is intracellular targeting of QDs in live cells.
➢ Field, L.D., Delehanty, J.B., Chen, Y.C. & Medintz, I.L. Peptides for Specifically Targeting nanoparticles to cellular organelles: Quo Vadis? *Acc. Chem. Res.* **48,** 1380-1390 (2015)	This article reviews intracellular targeting of nanoparticles including QDs using peptides as the targeting ligands.	This review points out the challenge of intracellular targeting of nanoparticles with peptide targeting ligands.
➢ Derfus, A.M., Chan, W.C.W. & Bhatia, S.N. Intracellular delivery of quantum dots for live cell labeling and organelle tracking. *Adv. Mater.* **16,** 961-966 (2004).	This paper systematically examined microinjection, electroporation and endocytosis-based delivery as the delivery method for intracellular targeted delivery of QDs. It was found that only microinjection could lead to targeting: peptide-conjugated QDs delivered by microinjection could lead to targeting to the cell nucleus or mitochondria in live cells.	Microinjection needs laborious and skillful operation; it's a serial process and is not scalable; it also needs instrument for delivery; with microinjection-based delivery, result reproducibility and cell viability are often problematic.
➢ Ruan, G., Agrawal, A.,	This paper imaged and tracked	It was found that the Tat

Marcus, A.I. & Nie, S. Imaging and tracking of Tat peptide-conjugated quantum dots in living cells: new insights into nanoparticle uptake, intracellular transport, and vesicle shedding. *J Am Chem Soc.* **47,** 14759-14766 (2007).	the cellular transport of Tat peptide-conjugated water-soluble QDs. The water-soluble QDs had a polymer coating; the electron microscopy size of these water-soluble QDs was > 10 nm in diameter.	peptide-conjugated QDs failed to enter the cell nucleus which is the target destination of Tat peptide, because they were trapped in intracellular vesicles.
➢ Tang, P.S. *et al.* The role of ligand density and size in mediating quantum dot nuclear transport. *Small* **10,** 4182-4192 (2014).	This paper systematically examined the effects of surface ligand density and particle size on the intracellular targeting effect, using the cell nucleus as the model target, of peptide-conjugated water-soluble QDs. Small molecule ligand mercaptoacetic acid was used for water-solubilization of QDs; the electron microscopy sizes of these water-soluble QDs were 3-8 nm in diameter.	It was reported that varying the surface density of peptide ligand led to different nucleus targeting specificity ranging from 20% to 60%.
➢ Yan, R. *et al.* Nanowire-based single-cell endoscopy. *Nat. Nanotechnol.* **7,** 191-196 (2012).	In order to bypass endocytosis in QD delivery, this paper developed a new cell injector by inserting a nanowire into a cell.	This new delivery method has all the limitations associated with conventional microinjection (see above). No targeting results were reported.
➢ Courty, S., Luccardini, C., Bellaiche, Y., Cappello, G. & Dahan, M. Tracking individual kinesin motors in living cells using single quantum-dot imaging. *Nano. Lett.* **6,** 1491-1495 (2006).	This paper reported delivery of kinesin-conjugated water-soluble QDs into cells by osmotic lysis of pinocytic vesicles.	It was reported that 13% of the conjugates had successful targeting to microtubules judging by directional motion driven by kinesin.
➢ Sun, C., Cao, Z.N., Wu, M. & Lu, C. Intracellular tracking of single native molecules with electroporation-delivered quantum dots. *Anal.Chem.* **86,** 11403-11409 (2014).	This paper reported delivery of anti-kinesin antibody-conjugated water-soluble QDs into live cells by an optimized electroporation technique which is based on a microfluidic device.	It was reported that ~5% of the intracellular QD conjugates were successfully targeted to kinesin. Instruments are needed for the delivery of QD probes.
➢ Katrukha, E. A. *et al.* Probing cytoskeletal modulation of passive and active intracellular dynamics using	This paper reported delivery of nanobody-conjugated water-soluble QDs into cells by an optimized electroporation	Electroporation needs instrument, often suffers from limited cell viability, result reproducibility and scalability,

nanobody-functionalized quantum dots. *Nature Communications* **8,** 14772 (2017).	technique to target motor proteins on cytoskeleton.	and requires considerable efforts in optimization in operation.
➢ Ma, Y.X. *et al.* Live cell imaging of single genomic loci with quantum dot-labeled TALEs. *Nature Communications* **8,** 15318 (2017).	This paper reported delivery of bioconjugated water-soluble QDs into the cell nucleus using the nucleus localizing sequence in the transcription-activator like effectors (TALEs). Inside the cell nucleus, the bioconjugated water-soluble QDs were reported to target to genomic loci.	It was reported that, after considerable optimization efforts, ~50% nucleus targeting specificity for the bioconjugated water-soluble QDs could be achieved. Inside the nucleus, the targeting specificity to genomic loci was not quantified, but judging from the images shown, the intra-nuclear targeting specificity was rather low.
➢ The present work.	A new intracellular targeted delivery technology for QDs based on new nanomaterial design is described.	With minimal optimization and using the cell nucleus as the model intracellular target, ~100% targeting specificity can be readily and reliably achieved. Inside the cell nucleus, Tat peptide conjugated QDs ("cS-bQD-Tat") could be largely accumulated to a specific location (nucleolus). This intracellular targeted delivery technology is also highly efficient, reproducible, convenient, scalable, and safe.

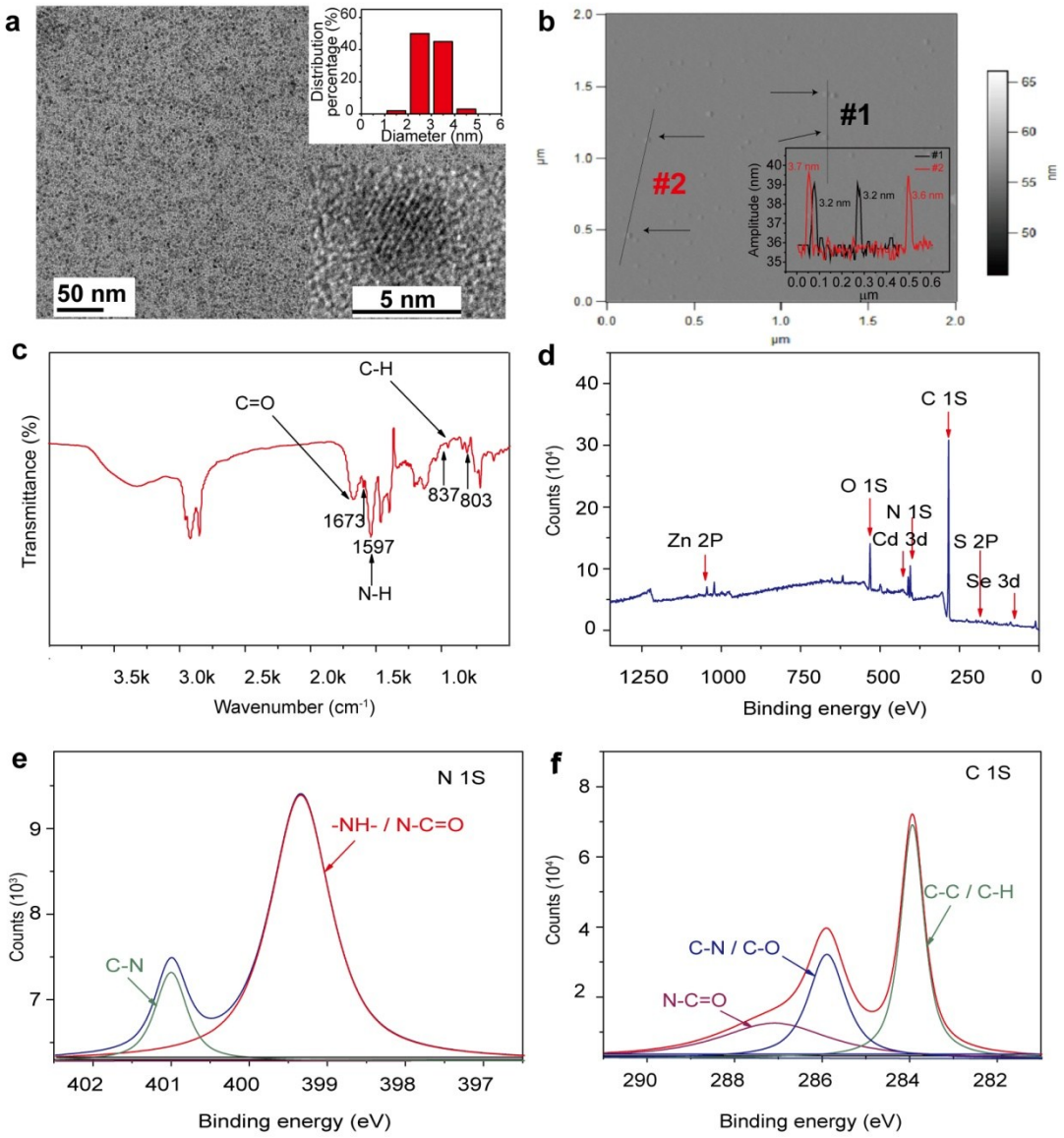

Supplementary Figure 1 Additional physico-chemical characterizations of cS-bQDs-Tat. (**a**) Transmission electron microscopy (TEM) characterization. The bottom-right inset shows a magnified view of a particle. The top-right inset shows the size distribution measured by TEM imaging (~200 particles were measured). (**b**) Atomic force microscopy (AFM) characterization. The bottom-right inset shows the surface height profiles along two lines in the AFM image. TEM and AFM results provide direct visualization of single particles with sub-nanometer resolution. (**c**) Fourier-transform infrared spectroscopy (FTIR) characterization. (**d-f**) X-ray photoelectron spectroscopy (XPS) characterization. The FTIR and XPS results provide chemical evidence (presence of characteristic spectroscopic peaks) of successful formation of the designed nanoprobes.

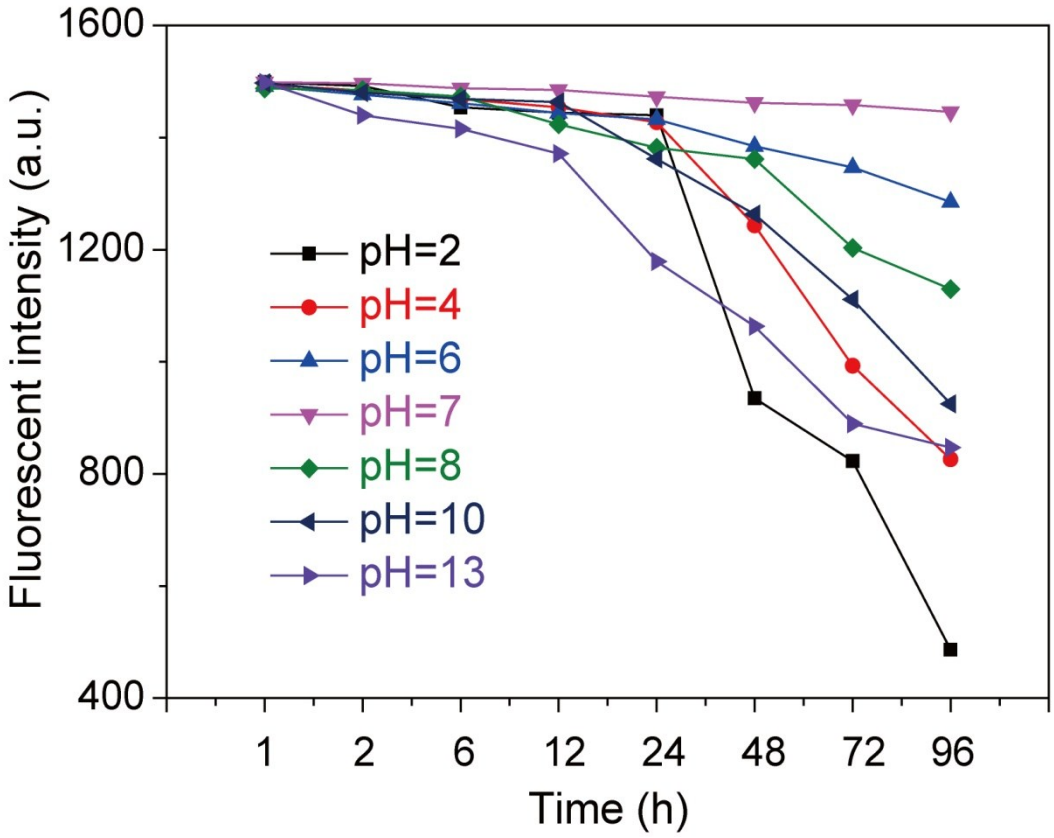

Supplementary Figure 2 pH stability of SDots-Tat in buffer solutions. The results indicate that SDots are most stable in pH neutral conditions. More acidic or more basic buffer conditions resulted in reduced fluorescence over time.

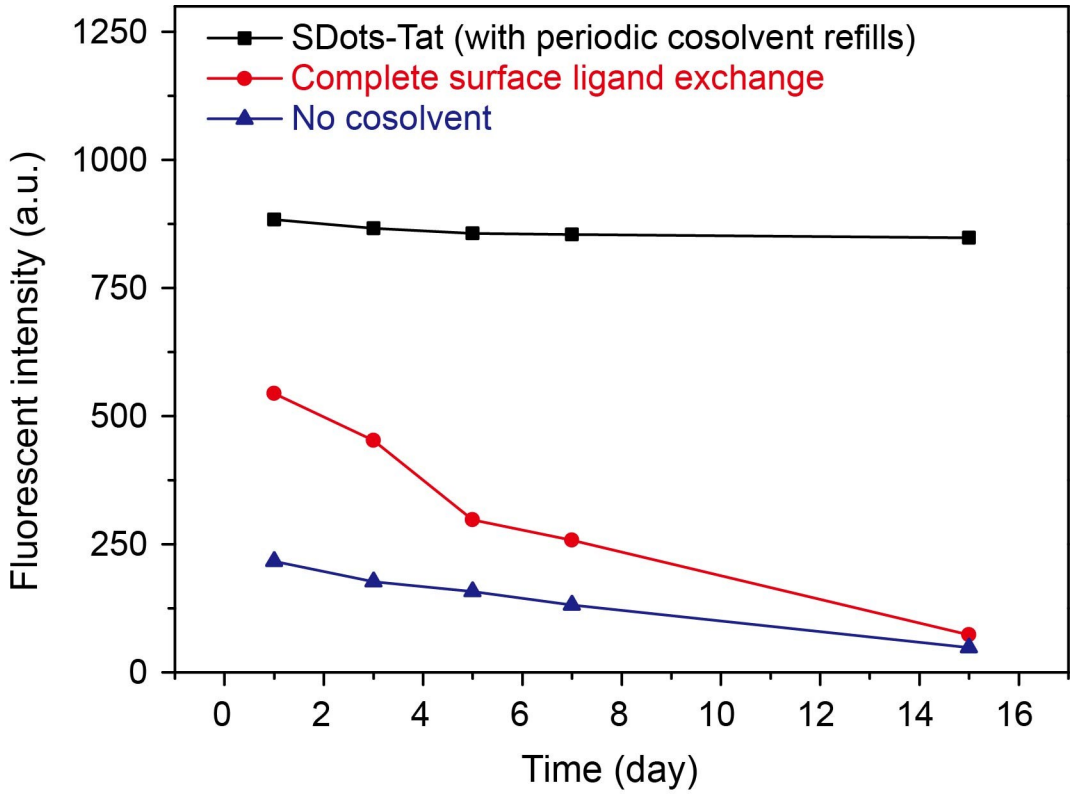

Supplementary Figure 3 Control studies for SDot surface chemistry development. Compared with the sample 'SDots-Tat' (bare hydrophobic QDs with a small percentage of surface ligands on the particle surface replaced by Tat peptide, in the presence of low percentage of cosolvent in water), the two control samples showed much lower fluorescence and after storage their fluorescence nearly disappeared completely. Identical amount of bare hydrophobic QDs was used to prepare the three different samples with different water-dispersion methods. The two control samples are 1) 'Complete surface ligand exchange', which is bare hydrophobic QDs (dispersed in water) with all the original ligands on the entire QD surface replaced by cysteamine, and 2) 'No cosolvent', which is bare hydrophobic QDs (dispersed in water) with a small portion of surface ligands replaced by cysteamine and without the use of any organic cosolvent, respectively.

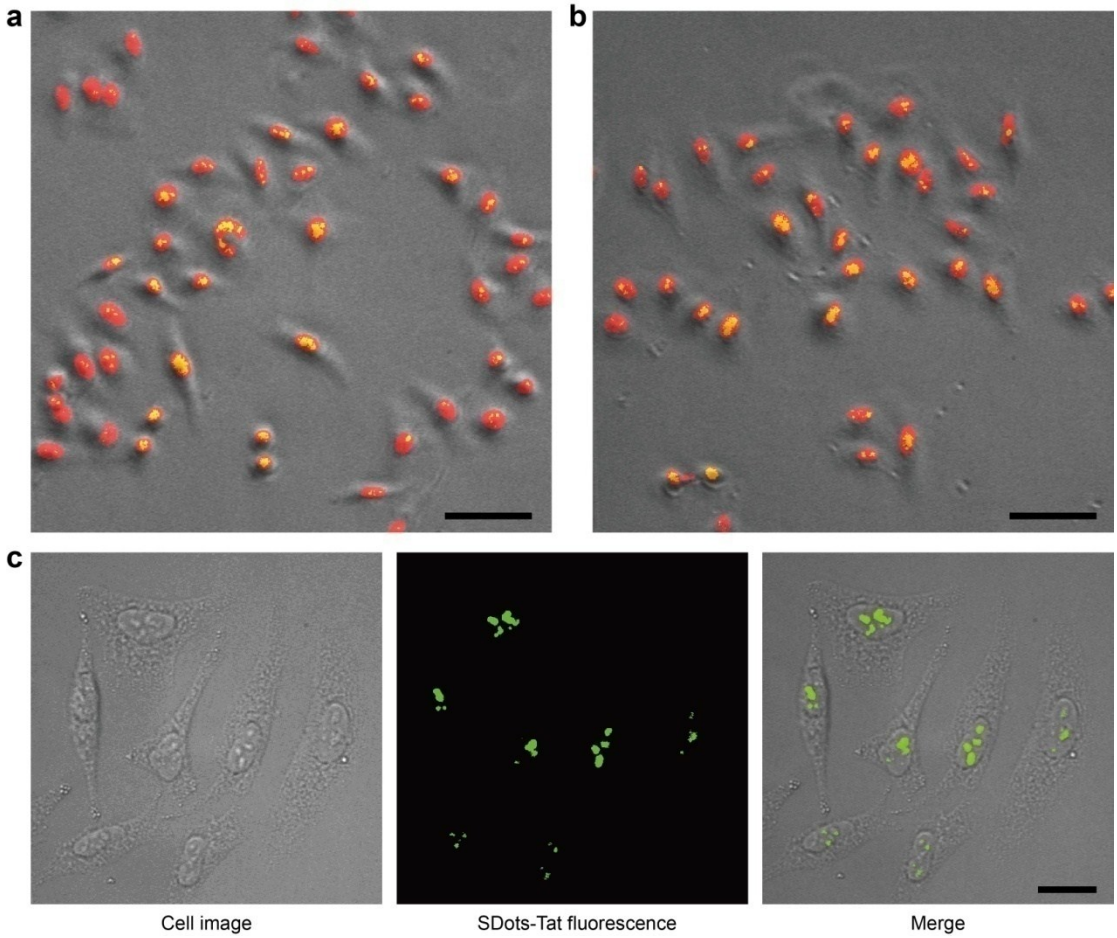

Supplementary Figure 4 Additional images of nucleus (more specifically, nucleolus) targeting of SDots-Tat in live cells. (**a,b**) Bird's-eye view light microscopy images of many HeLa cells with cS-bQDs-Tat successfully targeted to the cell nucleus with near-perfect targeting specificity. The magnification of the light microscopy objective used was 20×. The images are composites of bright field microscopy images, which show the cells, and fluorescent microscopy images, which show the cell nucleus (stained by the nucleus dye Hoechst 33342, red) and cS-bQDs-Tat (green). Colocalization of the cell nucleus and cS-bQDs-Tat leads to the composite color yellow. Scale bars, 60 μm. (**c**) Close-up view light microscopy image of HeLa cells with cS-bQDs-Tat successfully targeted to the cell nucleus, showing that inside the cell nucleus nearly all cS-bQDs-Tat are colocalized with the specific structure nucleolus. The magnification of the light microscopy objective used was 60×. Scale bar, 20 μm.

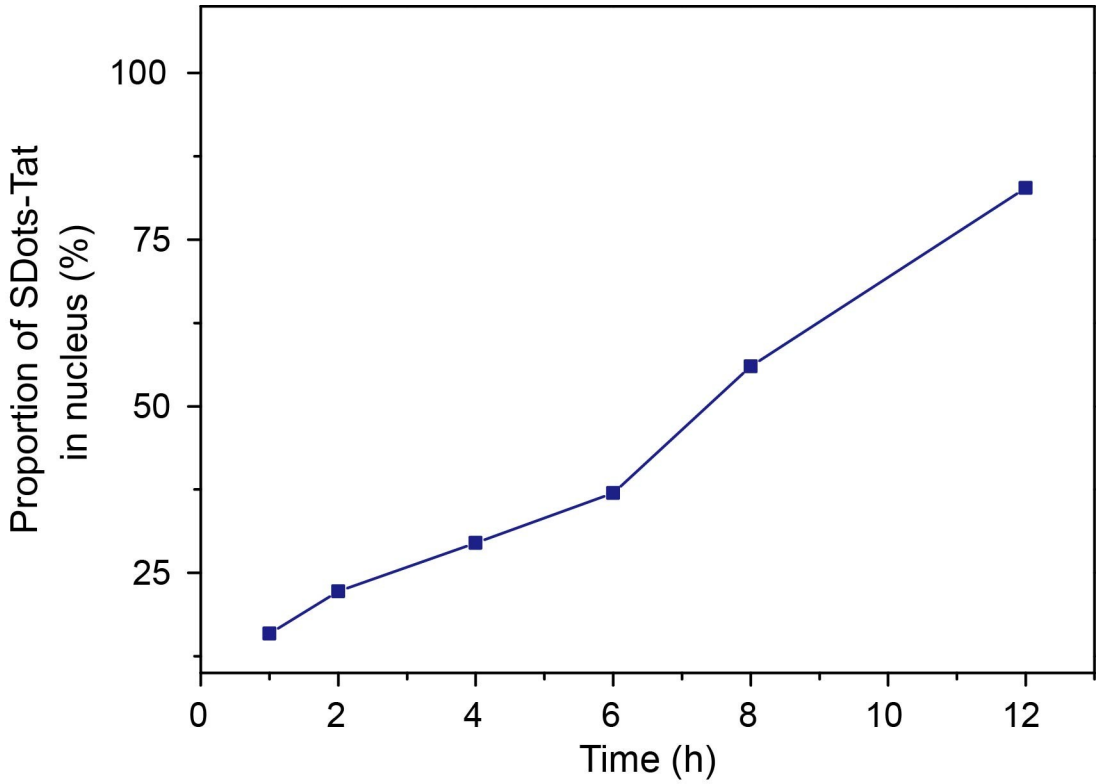

Supplementary Figure 5 Kinetics of targeted delivery of SDots-Tat to the cell nucleus in live HeLa cells as measured by fluorescent spectrometry of cell nucleus isolated from cell lysate at different time points of delivery. The results are in good agreement with those measured by confocal microscopy. The nanoparticle amounts measured by the nucleus isolation method are typically slightly lower than those measured by the confocal microscopy method due to loss of nanoparticles during the procedure of purifying cell nucleus from cell lysate.

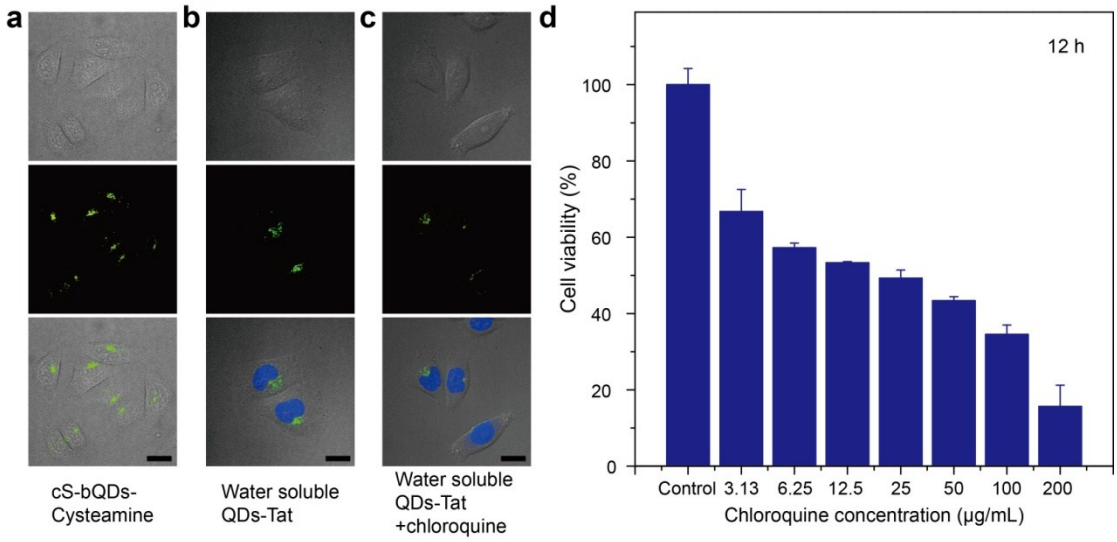

Supplementary Figure 6 Control studies on the intracellular targeting effect of cS-bQDs-Tat. In (**a**), cS-bQDs-cysteamine, i.e., SDots without the targeting biomolecule Tat peptide, didn't enter the cell nucleus, supporting that the nucleus targeting of cS-bQDs-Tat requires the biological function of Tat peptide. Scale bar, 20 μm. In (**b**), Conventional water-soluble QDs-Tat (hydrophobic QDs were water-solubilized with phospholipid-PEG micelles as described in the reference[34]; with the same number of Tat peptide per particle as that of cS-bQDs-Tat) didn't enter the cell nucleus, supporting the importance of the new nanoparticle design for intracellular targeting. Scale bar, 20 μm. In (**c**), the commonly-used vesicle-disrupting drug chloroquine (50 μM, or 16 μg/mL) was added for the conventional water-soluble QDs-Tat, and the results show that the use of chloroquine didn't significantly help the nucleus targeting. Scale bar, 20 μm. (**d**) shows that chloroquine causes serious cytotoxicity at the concentration range used for vesicle-breaking. HeLa cells were used for the cytotoxicity experiments. Error bars, mean ± s.e.m, $n = 5$.

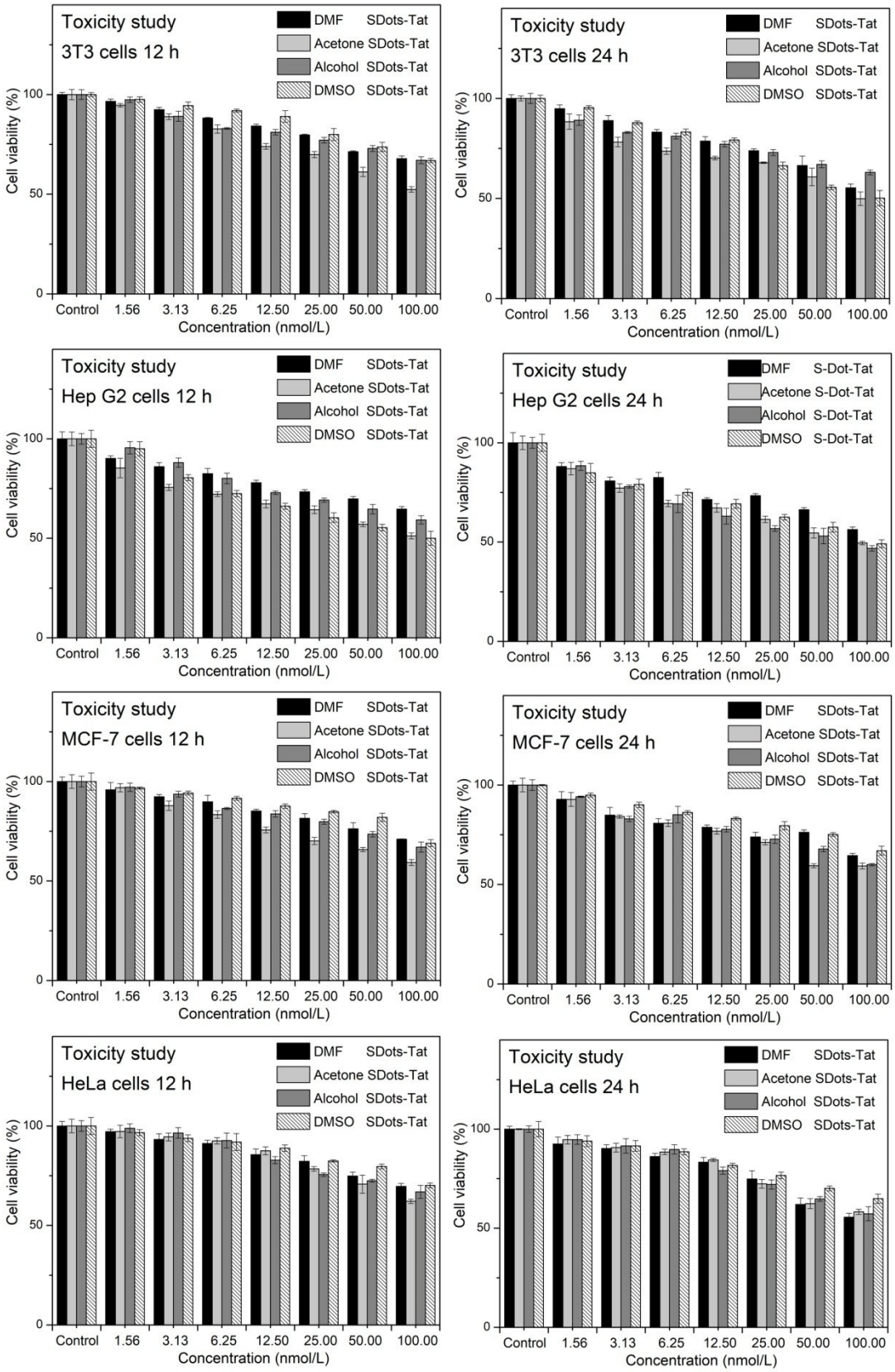

Supplementary Figure 7 Additional cell viability (MTT) study results. Different cell types, different cosolvent types, and different SDot concentrations were examined. The cosolvent concentration used was 1%.

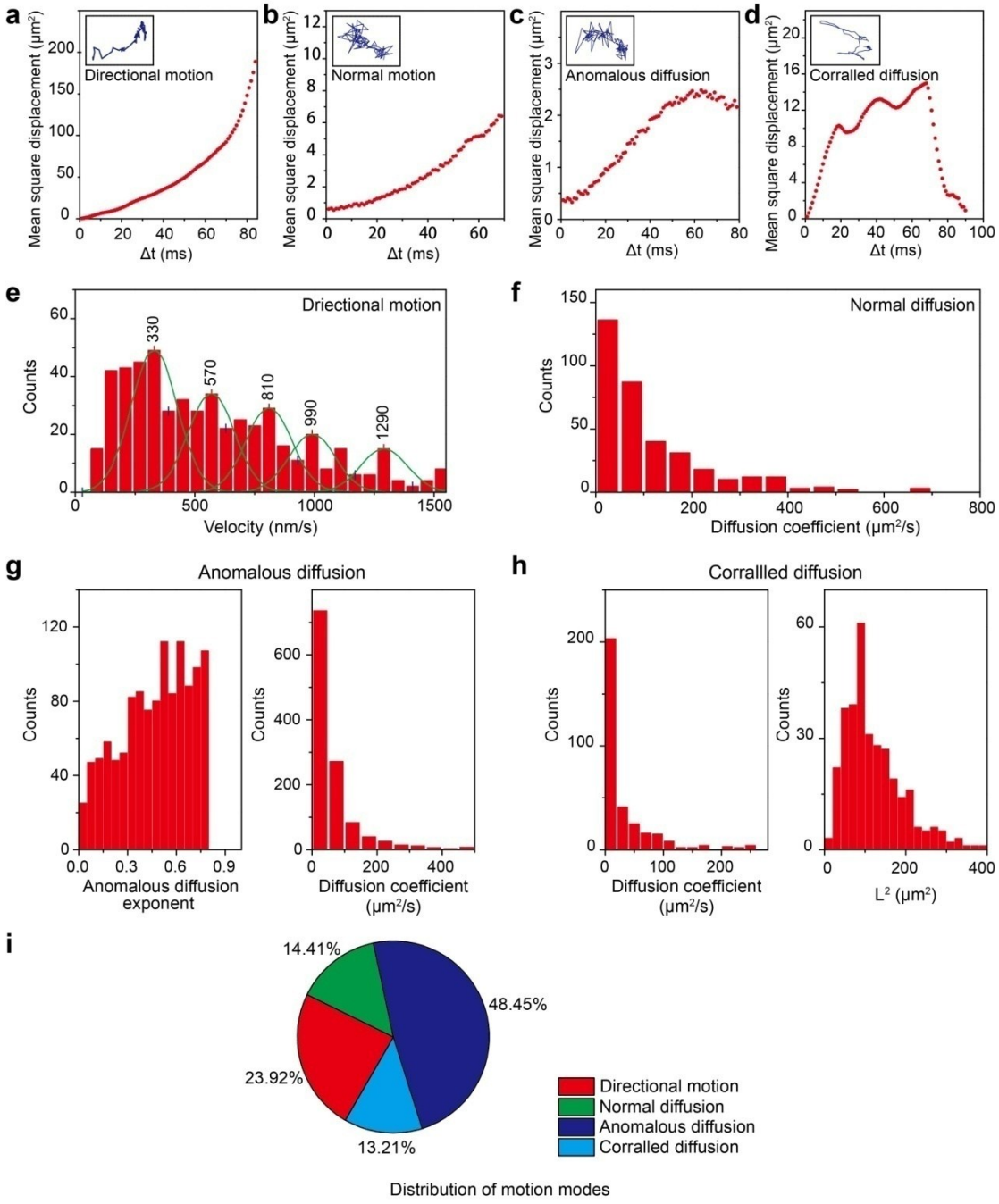

Supplementary Figure 8 Various motion modes of cS-bQDs-Tat in live HeLa cells found by single-particle tracking (SPT). (**a-d**) show the relation of mean square displacement (MSD) and time duration (Δt) for each of the four motion modes, namely directional motion, normal diffusion, anomalous diffusion, and corralled diffusion, respectively. The inset on the top-left corner in each of (a-d) shows a representative trajectory for the respective motion mode. (**e-h**) show the distributions of the characteristic constant(s) for each of the four motion modes, namely directional motion, normal diffusion, anomalous diffusion, and corralled diffusion, respectively. (**i**) shows the distribution of the four motion modes in the trajectories analyzed (~3000 trajectories).

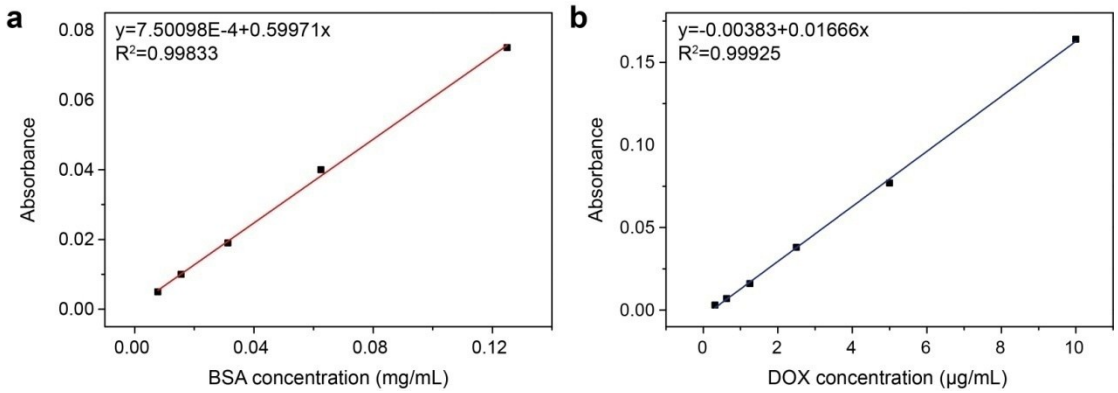

Supplementary Figure 9 Calibration curve for the concentration measurement of (**a**) bovine serum albumin (BSA) and (**b**) doxorubicin (DOX). The measurement was performed by UV-Vis absorption spectrometer at 280 nm for BSA and at 480 nm for DOX, respectively.

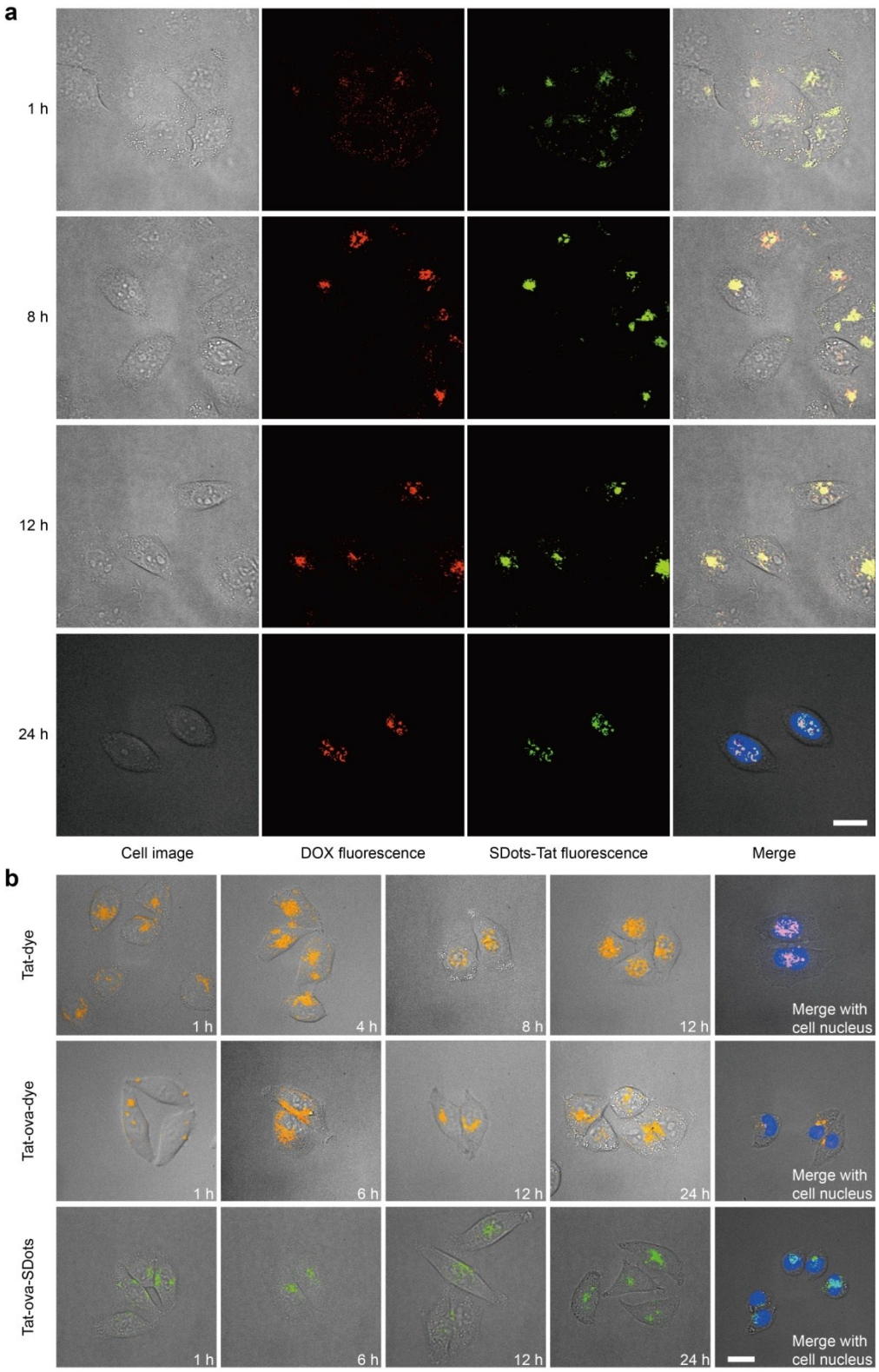

Supplementary Figure 10 Optical microscopy studies of SDots-Tat enhanced targeted delivery of (a) drug (doxorubicin, or DOX) and (b) macromolecule (ovalbumin, or ova). In (**a**), DOX gives red fluorescence, SDots-Tat gives green fluorescence, and the nucleus is fluorescently stained in blue color. The results show

that at all time points of the process of targeted delivery into the cell nucleus, DOX was mostly colocalized with SDots-Tat, with few of DOX detached from the nanoparticle surface during the targeted delivery process. Scale bar, 20 μm. (**b**) shows the time-dependent change of distribution of Tat-dye (no ova, the top row), Tat-ova-dye (the middle row), and Tat-ova-SDot (the bottom row), respectively. The results show that Tat-ova-SDots gives much better nucleus targeting effect than Tat-ova-dye. The formulation Tat-dye (no ova) is used as the positive control. Scale bar, 20 μm.

Supplementary Videos

Supplementary Video 1 Three dimensional reconstruction confocal images to show colocalization of SDots-Tat (green) with cell nucleus (blue, stained by the nucleus dye Hoechst 33342). Colocalization of the cell nucleus and cS-bQDs-Tat leads to the composite color watchet blue. 60× objective was used to capture the images.

Supplementary Video 2 Three dimensional reconstruction confocal images to show colocalization of SDots-Tat (green) with cell nucleus (red, stained by the nucleus dye Hoechst 33342). Colocalization of the cell nucleus and cS-bQDs-Tat leads to the composite color yellow. 20× objective was used to capture the images. More cells are shown in the view than Supplementary Video 1.

Supplementary Video 3 Representative video for single-particle tracking of SDots-Tat. 100× objective was used to capture the images. The rate of video capture was 25 frame/s.